

LOADS AND STRESSES IN ICF REACTORS

I. O. BOHACHEVSKY, L. A. BOOTH, T. G. FRANK, J. H. PENDERGRASS

*Los Alamos Scientific Laboratory, University of California,
P.O. Box 1663, MS 529, Los Alamos, New Mexico 87545, U.S.A.*

Abstract

The loads on inertial confinement fusion (ICF) reactor vessel walls resulting from anticipated operating conditions will consist of very intense but short duration mechanical and thermal pulses. In this paper these pulses are modeled and magnitudes of the associated impulses are estimated. Stresses induced in containment vessel walls are determined using engineering stress analysis. Simplifying assumptions required to derive analytic expressions for loads and stresses are made and the results are presented in a form convenient for parametric studies and determinations of design sensitivities to changes in different parameters. Results indicate that dominating mechanical design constraints may be determined by evaporation recoil, elastic buckling, or thermally excited stress waves. Technical topics that require additional theoretical and experimental studies for better ICF reactor modeling and more accurate assessment of their economic potential are identified.

1. Introduction

This paper summarizes the modeling of loads acting on and of stresses developed in the structure of an inertial confinement fusion (ICF) reactor vessel carried out as part of the Los Alamos Scientific Laboratory ICF reactor systems and applications studies.

There are three general approaches to stress analysis of explosion and microexplosion containment vessels:

- (1) Energy methods in which the explosion energy to be contained is equated to the strain energy that may be stored in the material of the containment vessel. This approach provides quick estimates of the amounts of materials required to contain a given energy release without the need to consider the technical details of the solution.
- (2) Mathematical theory of elasticity in which stresses and strains are determined as solutions of a boundary value problem for a system of partial differential equations and associated compatibility relations for a perfectly elastic medium. This approach provides deep insights into the behavior of elastic materials and opportunities to assess the implications and validity of different approximations used in the third, engineering, approach.
- (3) Engineering stress analysis in which simplifying assumptions are made about stress and strain distributions in structural elements based on empirical data and results of elasticity theory.

In situations where the postulates of perfectly elastic and continuous behavior may be locally violated without causing failure of the structural element, engineering stress analysis will approximate physical reality closer than elasticity theory.

In this paper we apply engineering stress analysis to estimate the loads that an ICF reactor vessel will have to withstand as a consequence of currently anticipated operating conditions and to derive expressions for the resulting stresses. We will emphasize approximations leading to explicit results from which parametric dependences and scaling relations are readily inferred. Results in this form are very useful in mathematical modeling of ICF reactor systems for cost studies and economic evaluations.

2. ICF Reactor Vessel Loads

2.1 ICF Reactor Design Requirements - ICF reactor concepts [1,2,3] are based on containment and utilization of repetitive explosive burn of fusion pellets (containing deuterium and tritium as fuel constituents) with energy released as 14-MeV neutrons (~75%), energetic fusion pellet debris composed of light and heavy element ions (~20%), and x radiation (~5%). Therefore the loads on the inner surfaces of the containment vessels will consist of intense but short duration pulses of x rays and ionized particles that typically penetrate only a few micrometers. In addition, the bulk of the structural materials will experience heating and atomic displacements damage induced by the highly penetrating neutrons. The operation of ICF reactors and fusion pellet energy release forms summarized above imply that the dominant considerations in ICF reactor design are: containment of several pellet microexplosions per second for extended periods of time, conversion of fusion energy (including energy from associated exoergic nuclear reactions) into usable forms, and breeding of the fuel constituent tritium with reactions between neutrons and lithium. These requirements can be satisfied by spherical or cylindrical reactor vessels surrounded by circulating liquid lithium contained between concentric structural shells.

In some designs [4] it appears advantageous to replace liquid lithium with solid lithium compounds, possibly encapsulated in pellets ranging in size from millimeter to centimeter.

2.2 ICF Reactor Vessel Loads - Various physical mechanisms generate loads acting on ICF reactor vessel walls. The nature of each mechanism is used to estimate magnitudes of these loads.

2.2.1 Evaporation Recoil - The pulse of x rays produced by a fusion fuel pellet microexplosion is absorbed in a thin layer of wall material, part of which may evaporate and thus generate an impulse at the wall. The magnitude of the recoil impulse per unit area, I_r , maximized with respect to the mass of material evaporated is given by [5]

$$I_r = \frac{Yx\eta}{4\pi R_1^2 \sqrt{2H}} \quad (1)$$

where Y is the total fuel pellet energy yield, x the fraction of energy in x rays, R_1 the inner radius of the vessel, H the heat of vaporization of the wall material, and η the effectiveness coefficient that accounts for the fact that not all vapor moves away from the wall with maximum attainable velocity. For a particular model of a Riemann wave expanding into vacuum, $\eta = 0.15$.

2.2.2 Impact of Pellet Debris - The kinetic energy of the high-velocity fuel pellet debris delivers to the vessel wall an impulse per unit area, I_d , whose magnitude is given by [5]

$$I_d = \frac{\sqrt{YfM}}{2\sqrt{2\pi R_1^2}} \quad (2)$$

Here M is the fuel pellet mass and f is the fraction of pellet yield appearing as debris kinetic energy. Equation (2) is a conservative estimate because it is based on the assumption that all the kinetic energy is converted into the impulse; in practice, part of the kinetic energy will appear as heat and will produce a recoil impulse whose magnitude can be estimated from Eq. (1) with an appropriate value for the energy fraction x. The two recoil impulses, however, cannot be combined because they occur at different times.

2.2.3 Blast Wave Reflection - When the ambient density in the cavity exceeds about 10^{14} atoms/cm³, the pellet microexplosion will generate a spherical blast wave. The impulse experienced by the reactor vessel wall during blast wave reflection is easily estimated as the product of the pressure at the wall behind the reflected wave, Eq. (7) of Ref. [5], and the pulse duration, which we approximate with the transit time of a sound wave through the shock compressed layer of the ambient cavity gas. The resulting expression for the impulse per unit area, I_b , is

$$I_b = \sqrt{\frac{3\gamma - 1}{8\pi}} \sqrt{\frac{Yf\rho_0}{R_1}} \quad (3)$$

where ρ_0 is the ambient mass density of the cavity medium and γ is the constant ratio of specific heats in that medium. In the derivation of Eq. (3), the Taylor-Sedov similarity description [6] of the blast wave was used. The validity of this solution deteriorates as the pellet mass increases and approaches the mass of the ambient cavity medium; at that

point, a modified blast wave theory [7] should be used to obtain accurate results. Unfortunately, any analysis of the blast phenomena that is more complex than the Taylor-Sedov description precludes the possibility of obtaining an analytic impulse estimate like Eq. (3).

2.2.4 Thermal Response of the Blanket - Lithium blankets, both liquid and solid compounds in pellet form, are designed to convert neutron kinetic energy into thermal energy and, therefore, will expand during reactor operation. The mean pressure increase caused by a confined expansion of a liquid lithium blanket is easily calculated to be [5]

$$p = \frac{\beta b}{c_\ell \rho_\ell} \frac{Y(1 - f - x)}{V}, \quad (4)$$

where p is the pressure increase, β the adiabatic bulk modulus, b the volume coefficient of thermal expansion, c_ℓ the heat capacity of liquid lithium, ρ_ℓ the density of liquid lithium, and V the blanket volume. This estimate is based on the assumption that neutron energy deposition is sufficiently slow or uniform and does not induce dynamic imbalances in the process. Actually, neutron energy is deposited with an exponentially decreasing intensity in a time that is short relative to the hydrodynamic response time. Therefore, it generates pressure waves in the liquid blanket. To analyze these waves and to model their effect, we solved the acoustic equations (in the plane wave approximation) for pressure, p , and velocity, u , perturbations in a liquid medium between two concentric shells shown in Fig. 1. The medium was initially at rest with an exponentially decreasing (from the inner shell R_1 to the outer shell R_2) pressure distribution induced by a postulated instantaneous neutron energy deposition with the scale depth λ ($\lambda \approx 70$ cm for liquid lithium). The details of the solution are presented in Ref. [8]; here we summarize the conclusions relevant to the present discussion:

- (a) The mean pressure rise and the first harmonic component account for nearly 90% of the deposited energy and therefore provide an approximate description of the phenomena that is adequate for the purpose of this paper;
- (b) The ratio of the amplitude of the first harmonic to the mean pressure rise increases nearly linearly with the nondimensional blanket thickness Δ/λ for values of $\Delta/\lambda < 4$, as shown in Fig. 2 where $\Delta = R_2 - R_1$. At the typical value of the blanket thickness $\Delta/\lambda \approx 1.6$, that ratio is approximately 0.50. Therefore, in stress calculations the mean pressure estimate given by Eq. (4) should be multiplied by a factor of ~ 1.50 to account for the transient overpressure.

To determine the effect of structural shell elasticity on pressure waves in the blanket, we solved the acoustic equations in the liquid medium coupled to the dynamic shell response equations [5] with the boundary conditions that specify the absence of cavitation at shell-blanket interfaces. Details of this solution are also described in Ref. [8]; here we summarize the results shown in Fig. 3. Plotted in this figure are pressure profiles in the blanket at different times. The upper-most curve corresponds to the time when the wave generated by the elastic response of the inner shell to an outward-directed pressure pulse arrives at the outer shell and the discontinuities in the subsequent profiles indicate the inward-traveling reflected wave. The amplitude of this wave is very small in comparison to the amplitude of the incident wave. Indeed, calculations for representative values of reactor parameters [8] show that the ratio of the impulses carried by the reflected and incident

waves is in the neighborhood of 0.04, which indicates that most of the original impulse is expended to accelerate the exterior shell. This circumstance greatly reduces opportunities for resonance.

Lithium blanket pressure may buckle or crush the inner shell. Buckling depends on the critical value of the pressure [5] and is independent of pulse duration within the framework of current failure models. Shell failure in compression (or tension) depends on the hydrodynamic impulse; its determination requires integration of pressure at the shell during the compression phase of the wave. We have carried out this integration explicitly for acoustic (linearized) wave motion and reported the results in Ref. [8].

2.2.5 Thermal Wall Loading - ICF reactor vessel walls experience two types of thermal loading: uniform steady-state temperature gradient across the wall thickness and pulsating surface temperature increases induced by the absorption of x rays and pellet debris ions. Our investigation of the latter phenomenon [9] showed that the surface temperature increase may be dominated by either heat conduction or heat capacity of the wall material and should be estimated with different expressions in these two different cases. The surface temperature increase, ΔT_s , is determined by heat conductivity when $\delta/2\sqrt{\kappa\tau} < 0.75$ where δ is the depth of penetration of x rays or ions, κ is the thermal diffusivity, and τ is the pulse duration. In this case, ΔT_s is given by

$$\Delta T_s = \frac{Yx}{2\pi R_i^2 \rho_{Si} c_{Si} \sqrt{\pi \kappa \tau}}, \quad (5)$$

where c_{Si} is the heat capacity and ρ_{Si} the density of the shell material.

When $\delta/2\sqrt{\kappa\tau} > 1.75$, the surface temperature is determined by heat capacity and is given by

$$\Delta T_s = \frac{Yx}{4\pi R_i^2 \delta \rho_{Si} c_{Si}}. \quad (6)$$

Clearly, the denominator is the heat capacity of the spherical shell of thickness δ .

When accurate results are required between the above two regimes, the exact solution of the appropriate heat transfer equation should be used [5,9].

3. Stresses in ICF Reactor Vessel Walls

The thermoelastic coupling constants for most materials of interest in ICF reactor design are very small [10] and, therefore, in preliminary analyses, stresses and temperature changes can be calculated independently. In our case this is true even for thermally generated elastic stress waves (as will be shown later) and, therefore, we neglect thermoelastic coupling. Because the primary effect of this coupling is to damp and disperse the elastic stress waves, our approach is conservative.

3.1 Membrane Stresses - The use of the thin shell approximation in stress calculations for the reactor vessel walls is justified because these walls will be thin relative to the vessel radius ($\delta_i/R_i < 0.01$, δ_i being the shell thickness) to avoid excessive neutron energy deposition and material cost. Because the wall loadings will be pulsed, the stresses must be determined from the analysis of dynamic shell response. To obtain conservative estimates that will remain valid when voids or bubbles develop in the liquid blanket or when the blanket is absent, we omit the hydrodynamic coupling term in the governing differential equation and thus obtain the following formulation [5]:

$$\frac{d^2 w_i}{dt^2} + \frac{2E_i}{(1-\nu)R_i^2 \epsilon_{si}} w_i = 0, \quad (7)$$

where w_i is radial shell displacement, E_i Young's modulus, ν Poisson's ratio, subscript $i = 1, 2$ denotes inner or outer shell, and t is time measured from impulse application. The initial conditions are specified by

$$w_i(0) = 0 \text{ and } \left. \frac{dw_i}{dt} \right|_0 = \frac{I}{\rho_{si} \delta_i}, \quad (8)$$

where I is the generic symbol for any of the previously estimated impulses I_r , I_d , or I_b . The above formulation is justified because the time during which the impulse, I , is delivered is very short relative to the period of natural shell vibration [5].

Denoting the stress by σ and the strain by ϵ and using the geometric compatibility relation $\epsilon_i = w_i/R_i$ together with the stress-strain relation $(1-\nu)\sigma = E_i \epsilon_i$, the solution of Eq. (7) results in the following expression for the tensile or compressive wall stress:

$$\sigma = \sqrt{\frac{1}{2(1-\nu)}} \frac{a_{si}}{\delta_i} I \sin\left(\sqrt{\frac{2}{1-\nu}} \frac{a_{si} t}{R_i}\right), \quad (9)$$

where a_{si} is the elastic wave speed given by $a_{si}^2 = E_i/\rho_{si}$. The maximum stress, σ_m , occurs when the fluctuating factor is unity and equals

$$\sigma_m = \sqrt{\frac{1}{2(1-\nu)}} \frac{a_{si}}{\delta_i} I. \quad (10)$$

When a particular expression for the impulse I (Eqs. 1, 2, or 3) is substituted into Eq. (10) and it is postulated that the shell thickness δ_i is determined by neutron transport requirements, Eq. (10) becomes a relation between the reactor vessel size, R_i , and the fuel pellet yield, Y . This relation is plotted in Fig. 4 for the three impulses considered and a steel containment vessel with 1-cm thick walls. Such results provide not only the required radius, but also indicate which type of load is critical in different yield regimes.

Membrane stresses induced by blanket thermal expansion and wave motion can be determined in a similar way once the integrated expression for the hydrodynamic impulse is derived. However, in this case the coupling term relating blanket pressure to shell velocity, dw_i/dt , should be included in Eq. (7) for consistency. We have solved this problem explicitly [5] and found that the solution requires tedious numerical evaluations and is not as convenient to use as Eqs. (1) through (3) with Eq. (10). Results obtained indicate that hydrodynamic coupling may reduce membrane stresses in some cases by as much as a factor of 10 [5]. In view of the awkwardness of the approximate solution, we are currently modeling the shell-blanket interaction numerically in exact, nonlinear formulation.

3.2 Elastic Buckling - A potential mode of failure for the inner shell is elastic buckling induced by hydrodynamic pressure in the liquid blanket. The critical pressure for that phenomenon is well known [11] and is given for spheres and cylinders, respectively, by

$$p_{cs} = \frac{2E_1\delta_1^2}{R_1^2 \sqrt{3(1-\nu^2)}} \quad \text{and} \quad p_{cc} = 0.807 \frac{E_1\delta_1^{5/2}}{LR_1^{3/2}} (1-\nu^2)^{-3/4}, \quad (11)$$

where L is the unsupported cylinder length. When the expression for the blanket pressure given by Eq. (4) (with the necessary factor to account for the transient overpressure determined in Ref. 8) is used in the above equations, they also become relations determining the required vessel radius for a given fuel pellet yield and shell thickness. For a spherical vessel and for the approximation $V = 4\pi R_1^2 \Delta$, that relationship does not contain the radius R_1 and therefore should be viewed as a constraint on the shell thickness δ_1 imposed by the pellet yield Y.

3.3 Thermal Stresses - Thermal stresses arise because thermal distortions in different parts of the shell are, in general, incompatible. In the thin-shell approximation and with the hypothesis that the temperature inside the wall varies linearly, a steady-state temperature difference ΔT across the wall induces a stress of magnitude [5]

$$\sigma = \frac{E_1 \alpha_1 T}{2(1-\nu)}, \quad (12)$$

where α_1 is the coefficient of linear thermal expansion.

An instantaneous surface temperature increase ΔT_s induces a local thermal stress of twice that magnitude [5],

$$\sigma = \frac{E_1 \alpha_1 \Delta T_s}{1-\nu}. \quad (13)$$

Substituting into this equation an appropriate expression for ΔT_s from either Eq. (5) or Eq. (6) would again result in a relation between vessel radius R_1 and pellet yield Y if the allowable value of the stress σ_m for these conditions were known. However, because the surface temperature increase given by Eqs. (5) and (6) will persist for only approximately 10^{-9} s and will be localized to a depth of less than a few micrometers, it is not clear that a catastrophic failure would occur if the surface material yields locally or even melts for such a short time. Clearly, theoretical and experimental investigations are needed to determine allowable values of the stress to be used in Eq. (13) for the loading characteristics indicated above.

3.4 Elastic Stress Waves - A possible approach to the determination of allowable transient thermal stress is through the analysis of elastic wave propagation in the vessel wall. A surface layer of depth δ heated sufficiently rapidly to a high temperature does not have time to expand and consequently experiences a compressive stress σ_0 that is relieved with a stress wave, rather than by heat conduction. This can be seen from the following simple estimates. The characteristic time to propagate the effect elastically through a distance δ is given by $t_w \approx \delta/a_{s1}$; for steel and $\delta \approx 10^{-4}$ cm, $t_w \approx 2 \times 10^{-10}$ s. The characteristic time for heat conduction is $t_c \approx \delta^2/\kappa$; for the same material and δ , $t_c \approx 2 \times 10^{-7}$ s. Hence the effect of the thermal pulse will propagate elastically approximately a thousand times faster than by conduction.

Instead of giving a standard mathematical description of wave propagation we summarize the characteristics of thermally excited stress waves graphically in Fig. 5. Shown schematically is the initial compressive stress σ_0 induced by the temperature increase ΔT_s in

the surface layer of depth δ , the resulting stress wave during reflection from the inner face of the wall, and the same wave at the time δ/a_{s1} when the reflection process is completed. The resulting wave propagating through the wall consists of a compression phase of length δ , followed by an equally long tensile phase, the amplitudes of both phases being equal to $\sigma_0/2$. Clearly, this wave produces tensile and compressive stresses equal to $\sigma_0/2$ at the inner and outer faces of the wall and, therefore, its amplitude should be limited to an allowable stress level to avoid spallation.

Denoting the allowable stress by σ_m as in Sec. 3.1, and using Eq. (6) in Eq. (13) to obtain the expression for σ_0 , we arrive at the following relation between the radius of the inner shell, R_1 , and the pellet yield Y :

$$R_1 = \sqrt{\frac{E_1 \alpha_1 X Y}{8\pi(1-\nu)\delta\rho_{s1}c_{s1}\sigma_m}} \quad (14)$$

This estimate, however, may be excessively conservative because it does not account for the fact that some of the initial thermal energy may be used to melt and vaporize the surface material and that elastic waves may be damped significantly by internal friction of the material. Even though the thermoelastic coupling constant and therefore the logarithmic decrement are small, the cumulative effect is not negligible when the ratio $a_{s1}\delta/2k$ is very large [10], which is the case for reactor vessel walls. Also, the analysis is not very useful unless the value of δ is known. To resolve uncertainties associated with this problem, we are investigating thermal generation and propagation of elastic stress waves numerically with realistic equations of state and stress-strain relations.

3.5 Fatigue - Cyclic operation of ICF reactors implies that fatigue strength (with appropriate safety factors) should be used as the allowable working stress. Fatigue strength is determined by threshold values of stress concentrations at microscopic fatigue cracks and equals that value of the stress at which the rate of growth of the size of fatigue cracks vanishes for all practical purposes.

If thermally generated elastic stress waves are determined to be the governing phenomenon in the design of ICF reactor vessels [Eq. (14)], then the usual fatigue strengths of materials may be increased because of extreme shortness of wavelengths of these waves. In a recent paper, Weertman [12] pointed out that current theories of fatigue failure may not be valid when the stress wavelength is smaller than the fatigue crack and proposed an appropriate formulation. Results of his modified formulation indicate that increased levels of fluctuating stresses may be tolerated when stress wavelengths are very small. This area requires additional study.

4. Concluding Remarks

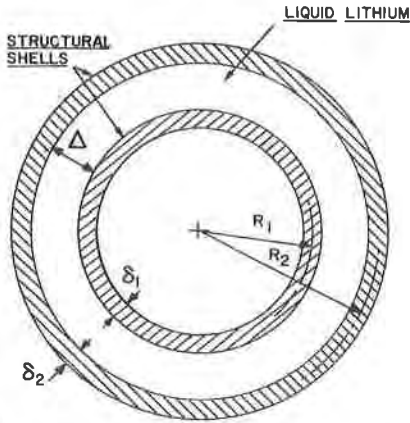
ICF reactor studies are now in conceptual design stages when, rather than performing accurate design calculations, it is preferable to ensure that potential mechanisms of failure and degradation are adequately investigated and bounds on relevant design parameters are determined. We therefore directed our efforts towards obtaining results that indicate sensitivities of specific designs to different parameters. Our work achieved that purpose; results exemplified by Eq. (14) and illustrated in Fig. 4 show the explicit dependence of the reactor vessel radius on each parameter and indicate potential payoffs that can be expected from optimizations of different parameters.

The results are also helpful in determining critical loading mechanisms in different parameter ranges and in identifying topics which require additional investigations to better model ICF reactor performance. Some of these topics are: determination of allowable stresses for loadings with very short (10^{-9} s) and shallow (submicron) thermal pulses, an appropriate fatigue failure model for materials stressed with elastic waves of submicron wavelength, determination of critical buckling pressures for transient loads of less than a millisecond duration, and analytical models for vessels with ribs, flanges, and openings.

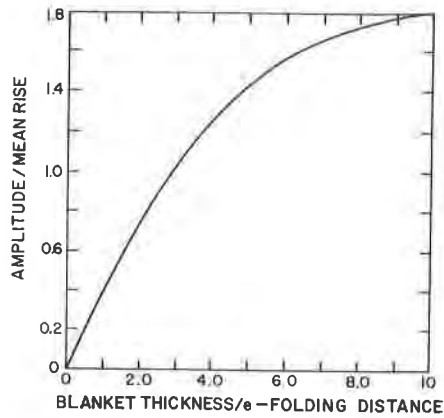
Not mentioned in this paper, but of critical importance also, is study of the effects of pulsed neutron damage on material properties in the appropriate range of neutron energy (~ 14 -MeV) and fluence.

References

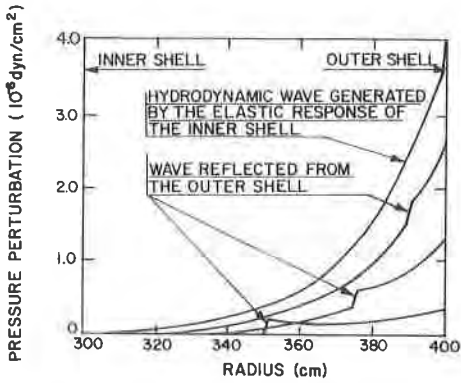
- [1] BOOTH, L. A., FREIWALD, D. A., FRANK, T. G., and FINCH, F. T., "Prospects for Generating Power With Laser-Driven Fusion," Proc. IEEE 64(10), 1460-1482 (October 1976).
- [2] FRANK, T. G., FREIWALD, D. A., MERSON, T., and DEVANEY, J. J., "A Laser Fusion Reactor Concept Utilizing Magnetic Fields for Cavity Wall Protection," Proc. 1st Topical Meeting on Techn. of Cont. Nucl. Fusion 1, 83 (1974).
- [3] MANISCALCO, J. A., MEIER, W. R., and MONSLER, M. J., "Conceptual Design of a Laser Fusion Power Plant," Lawrence Livermore Laboratory report UCRL-79652 (July 1977).
- [4] CONN, R. W., et al, "SOLASE, a Conceptual Laser Fusion Reactor Design," Univ. of Wisc. Fusion Res. Program report UWFDM-220 (December 1977).
- [5] BOHACHEVSKY, I. O., "Scaling of Reactor Cavity Wall Loads and Stresses," Los Alamos Scientific Laboratory report LA-7014-MS (November 1977).
- [6] KOROBEJNIKOV, V. P., Problems in the Theory of Point Explosion in Gases, Nauka, Moscow (1973).
- [7] FREIWALD, D. A., and AXFORD, R. A., "Approximate Spherical Blast Theory Including Source Mass," J. Appl. Phys., 46(3), 1171-1174 (1975).
- [8] BOHACHEVSKY, I. O., "Hydrodynamic Waves in Liquid Lithium Blanket," in "Laser Fusion Program Progress Report, July-December 1977," Los Alamos Scientific Laboratory report LA-7328-PR (December 1978).
- [9] FRANK, T. G., BOHACHEVSKY, I. O., BOOTH, L. A., AND PENDERGRASS, J. H., "Heat Transfer Problems Associated with Laser Fusion," AICHE Symp. Ser. 73(168), 77-85 (1977).
- [10] ACHENBACK, J. D. Wave Propagation in Elastic Solids, North Holland, Amsterdam (1973).
- [11] ROARK, R. J. Formulas for Stress and Strain, McGraw-Hill, New York (1965).
- [12] WEERTMAN, J., "Theory of Irradiation Induced Growth of Fatigue Cracks," J. Nucl. Mate. 55, 253-258 (1975).



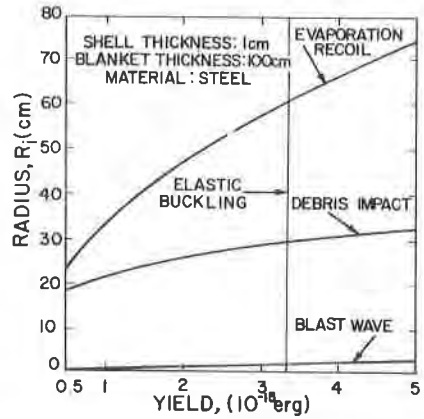
1. Spherical ICF reactor vessel.



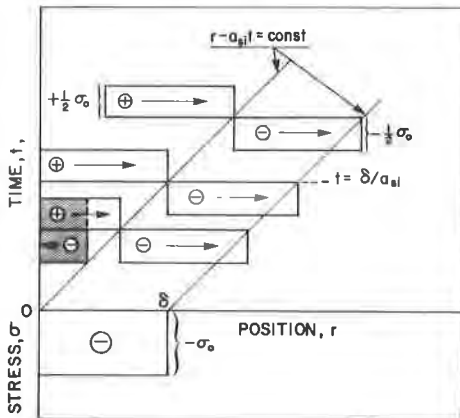
2. Relative amplitude of the first harmonic component of the pressure wave in the blanket.



3. Wave reflection from the outer shell.



4. Radius-yield relations for ICF reactor vessels determined by structural strength requirements.



5. Stress wave propagation: + tensile, - compressive.